Open micro-fluidic system for atomic force microscopy-guided *in situ* electrochemical probing of a single cell

WonHyoung Ryu,*[a] Zubin Huang,[a] Joong Sun Park,[a] Jeffrey Moseley,[b] Arthur R. Grossman,[b] Rainer J. Fasching[a] and Fritz B. Prinz[a,c]

Received 28th February 2008, Accepted 3rd June 2008
First published as an Advance Article on the web 25th July 2008
DOI: 10.1039/b803450h

Ultra-sharp nano-probes and customized atomic force microscopy (AFM) have previously been developed in our laboratory for *in situ* sub-cellular probing of electrochemical phenomena in living plant cells during their photosynthesis. However, this AFM-based electrochemical probing still has numerous engineering challenges such as immobilization of the live cells, compatibility of the immobilization procedure with AFM manipulation of the probe, maintenance of biological activity of the cells for an extended time while performing the measurements, and minimization of electrochemical noise. Thus, we have developed an open micro-fluidic channel system (OMFC) in which individual cells can be immobilized in micro-traps by capillary flow. This system affords easy AFM access and allows for maintenance of the cells in a well-defined chemical environment, which sustains their biological activity. The use of micro-channels for making the electrochemical measurements significantly reduces parasitic electrical capacitances and allows for current detection in the sub-pico-ampere range at high signal bandwidths. The OMFC was further studied using simulation packages for optimal design conditions. This system was successfully used to measure light-dependent oxidation currents of a few pico-amperes from the green alga *Chlamydomonas reinhardtii*.

Introduction

Photosynthesis in plant cells is a ubiquitous natural solar energy conversion process. Light energy is captured by light harvesting complexes, which funnel that energy into the reaction centers of the photosynthetic electron transport chain, causing a charge separation that provides the driving force to split water into protons, electrons, and oxygen. The electrons are passed along an electron transport chain, where the energy generated during electron flow can be used for ATP formation and the reduction of inorganic carbon (but also sulfate and nitrite reduction).[1] This process is very similar to the energy process of solar cells and has the potential to be exploited by direct extraction of energetic electrons from the photosynthetic electron transport system. We hypothesized that insertion of micro/nano-electrodes proximal to the electron transport chain housed in the photosynthetic membranes would help reveal fundamental mechanisms associated with electrochemical reactions inside the cell.[2,3]

Extraction of electrochemical energy from the photosynthetic apparatus would require insertion of electrodes into living cells that are maintained in a well-defined micro-environment, and would cause disruption of natural photosynthetic electron flow. This local electrochemical probing of living cells raises several technical challenges including: (1) fabrication of ultra-sharp probes for non-destructive cell penetration; (2) nano-scale manipulation of probes; (3) electrodes with sufficient electron affinity; (4) immobilization of cells at single cell resolution; (5) maintenance of cell viability during the experiments; (6) reduction of exogenous electrochemical noise, which interferes with the measurements. Our laboratory and other researchers have successfully used atomic force microscopy (AFM) controlled nano-electrodes of sufficient electron affinity to carry out electrochemical analysis,[4–6] addressing the first three technical challenges of our goal to extract electrical energy from photosynthesis. However, challenges regarding optimal cell manipulation and the elimination of measurement noise had not been solved.

The target cell for this investigation is the unicellular, green alga *Chlamydomonas reinhardtii* (designated Chlamydomonas throughout), which unlike mammalian cells, does not adhere to the surface of most substrates. Since internal or external AFM-probing of cells requires a physically stable adhesion to a substrate, it was necessary to develop a robust immobilizing method for non-adherent cells. Algae have been immobilized in a gel matrix,[7] as shown in Fig. 1(a). However, this gel-based immobilization is incompatible with AFM probing since the penetration and navigation of AFM probes within the gel matrix are very limited. Micro-fluidic systems have also been explored in order to immobilize non-adherent cells. Previous investigations have used hydrodynamic force,[8–12] negative pressure,[13–15]

[a]*Rapid Prototyping Laboratory for Energy and Biology, Department of Mechanical Engineering, Stanford University, Stanford, CA, 94305. E-mail: whryu@stanford.edu; Fax: +1 (650) 723-5034; Tel: +1 (650) 723-6488*
[b]*Department of Plant Biology, Carnegie Institution of Washington and Department of Biological Sciences, Stanford University, Stanford, CA, 94305*
[c]*Department of Material Science and Engineering, Stanford University, Stanford, CA, 94305*

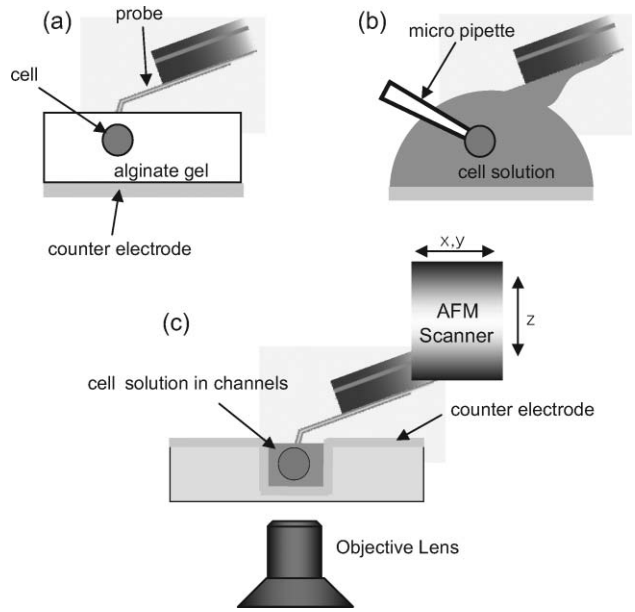

Fig. 1 Diagrams of immobilization scheme for nano-probe measurements on living cells. (a) Cell immobilized in gel system; (b) cell in solution; (c) cell immobilized in micro-fluidic structure.

centrifugal force,[16] or artificial tethering by antigens or resins.[17–20] Furthermore, adhesion-independent patterning methods such as electrophoresis,[21] dielectrophoresis,[22] and optical techniques[23,24] have also been employed. However, these methods either require a 'closed' micro-fluidic system, which is incompatible with AFM probing, or the complex system architectures.

Most AFM investigations, mainly for probing the topography of cells/structures, perform the scan in an aqueous environment.[25,26] However, as shown in Fig. 1(b), this aqueous environment becomes a large source of unwanted capacitive currents that interfere with the electrochemical probing, since the magnitude of the capacitive leakage current is directly proportional to the wetted area of a nano-probe. Paradoxically, the target cells of the experiment must be kept fully hydrated to maintain their viability. Therefore, it has been necessary to develop a method to maintain the level of the aqueous solution at the minimum that sustains survival of target cells during electrochemical monitoring. The requirements of the system also include open access for AFM probing, maintenance of convenient and rapid solution exchange, and a low cost, easy method for fabrication.

Here, we propose the use of microfluidic channels that immobilize single cells by a capillary force and allow open access to the AFM-linked probe. A proper choice of the dimensions of the open micro-fluidic channels minimizes the leakage current through the capacitive pathways of the wetted AFM probes while maintaining viability of subject cells. The cells are carried from a dispensing port by capillary flow and sequentially immobilized in micro-traps within open micro-channels. This system facilitates immobilization of multiple cells in an arrayed format such that AFM probing of the different cells is possible without changing the immobilization plateform. For this study, we employed micro-molding to construct micro-channels on polymethyl methacrylate (PMMA) layers. The micro-molded channel structures were sputter-coated with gold and surface-treated using thiolated polyethylene glycol (PEG-SH) in order to enhance capillary flow. We optimized the geometry of micro-traps for the maximum trapping yield using a finite element analysis (FEA) method. Cells of our model photosynthetic alga, *Chlamydomonas reinhardtii*, were effectively immobilized in the optimized micro-channel structures. Furthermore, we successfully penetrated the cells with nano-probes that were positioned at the cell surface with guidance provided by the AFM system. In addition, light-signal dependent electrochemical response from a *Chlamydomonas reinhardtii* was observed demonstrating the feasibility of nano-scale electrochemical analysis.

Materials and methods

1. Concept of capillary trapping

Micro-fluidic technology has been extensively explored to immobilize various biologics from proteins to cells. However, most micro-fluidic platforms are closed systems that do not allow access of nano-probes (AFM operated) to the immobilized biological samples. Our objective was to develop a micro-fluidic platform that allowed open access of nano-probes and immobilization of single cells or organelles while maintaining a physically and chemically controlled environment. Furthermore, it was necessary to incorporate *in situ* exchange of chemical environments in the micro-fluidic structures in order to examine the consequences of modulating photosynthetic activity on the generation of electrochemical gradients.

The current configuration used to make the measurements presented in this manuscript is illustrated in Fig. 1(c). Single algal cells are immobilized by capillary flow at the micro-traps in open micro-channels on an optically transparent PMMA substrate, as shown in Fig. 2. A nano-probe is then moved to the top surface of the target cell by AFM manipulation. The nano-probe is then lowered onto the surface membranes and the sharp tip of the probe penetrates that membrane; the membrane then adheres to the hydrophobic surface that coats the probe, generating a tight seal that prevents leakage of the intracellular content into the surrounding medium. Optical, force, and electrochemical signals are then monitored and recorded *in situ* as the probe is positioned at the various locations in the cell.

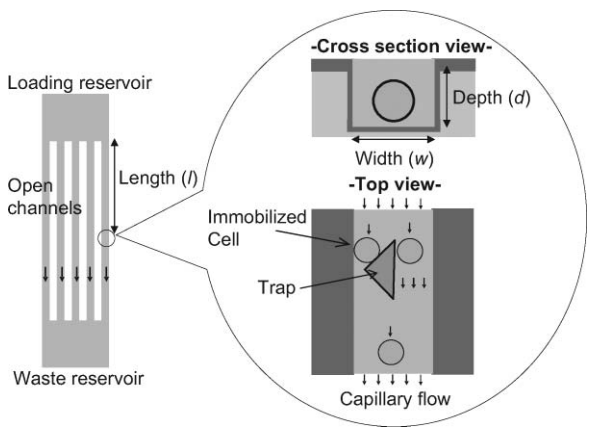

Fig. 2 Immobilization of a single cell in a micro-trap by a capillary flow in open micro-channels.

2. Theory of capillary flow in open channels

Capillary pressure in the flow direction (z) of open micro-channels can be described as

$$P_{c,z} = \gamma\left(\frac{\cos\alpha_b}{d} + \frac{\cos\alpha_l + \cos\alpha_r}{w}\right) \quad (1)$$

where γ is the surface tension of a liquid, $\alpha_{b,l,r}$ are the contact angles of the liquid on the bottom, left, and right wall, respectively, and d and w are the depth and width of a micro-channel.[27] As this channel is open at the top, there is no contribution of a top interface (liquid/air) to capillary pressure in the flow direction (z). The volume flow rate (Q) and flow resistance (R_{fr}) in the micro-channels are expressed as[28]

$$Q = \frac{1}{\eta}\frac{\Delta P}{R_{fr}} \quad (2)$$

$$R_{fr} = \frac{12L}{R_h^2 A}(1 - 1.3553a + 1.9467a^2 - 1.7012a^3 + 0.9564a^4 - 0.2537a^5) \quad (3)$$

where η is the viscosity of the liquid, ΔP is the difference of pressure between the two liquid fronts, L is the filled length of the channel, R_h is the hydraulic radius of the channel, A is the cross-sectional area of the channel, and a is the aspect ratio of the channel. The aspect ratio is defined as either height/width or width/height such that $0 \le a \le 1$. In our experiment, ΔP is equal to $P_{c,z}$ from eqn (1) since the dispensing port has a relatively large wetted perimeter compared to the micro-channels.

3. Fabrication

The silicon mold fabrication process was mainly composed of one lithography step and one etching step (Fig. 3). Photoresist (AZ 3612, Shipley, MA) was spun on the wafer with the thickness of 1.6 μm and channel features were patterned by lithography. The patterned photoresist was hardened by baking in 110 °C oven for 30 min. Thereafter, the wafer was etched down to either 8 μm deep for 20 μm wide channels or 20 μm deep for 80 μm wide channels by deep reactive ion etching (DRIE) to form the mold structure. The photoresist was then removed by 3 min oxygen plasma and 20 min piranha at 120 °C. Teflon (Teflon AF, 400S1-100-1, Dupont, DE) was coated on top of Ti (50 nm thick) on the patterned silicon molds to enhance demolding.

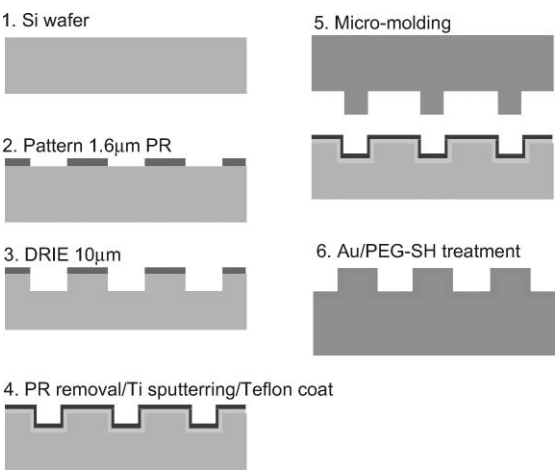

Fig. 3 Fabrication process used to construct open micro-fluidic channel system.

PMMA hot embossing was done on a Carver press.[29] The 4 inch silicon wafer mold was placed between two parallel hard substrates. A 50 μm thick PMMA film was placed on the top of the micro-fabricated silicon mold (Fig. 3). The whole structure was heated to 140 °C and 1400 lb of force was applied over the 4 inch silicon mold for 5 min, after which it was cooled to room temperature and the PMMA film was de-embossed. The final product of this process was a channel structure with a width of 20 μm and a depth of 5 to 10 μm.

After completing the molding, the polymeric film was cut into eight micro-fluidic devices (16 × 30 mm^2). Each device was cleaned in an ultrasonic bath for 5 min and sputter-coated with Au (about 30 nm thick) at 20 mA for 4 min to achieve a resistance of less than 100 ohms across the device surface. The device was then immersed in an ethanolic solution of thiolated polyethylene glycol solution (mPEG-SH, NanoCS, NY, 5 mg ml^{-1}) for 10 min to form a self-assembly monolayer on the gold, generating a hydrophilic surface that would facilitate capillary flow. The device was finally cleaned with deionized water and blown dry. The surfactant treatment effectively reduced the contact angle to below 30°.

4. Set-up and device operation (confocal/AFM setup)

The AFM Picoplus 5.3.3 system (Molecular Imaging, USA) was custom-fitted on top of the sample stage of a Zeiss Confocal Microscope (Zeiss LSM, USA). A nano-probe was attached to the AFM scanner by custom-fabricated AFM nozzle.[5] The nano-probe had the needle shape (20 to 50 μm long and the end radius of 50 nm) made of silicon nitride (300 nm thick) layer. A thin gold (100 nm thick) layer was embedded between the silicon nitride layers as an electrode material. A micro-channel substrate for cell immobilization was mounted on the AFM sample stage. Typically, a single substrate contained three identical groups of channels for multiple experiments. A cell solution (3 μL) was dispensed into a dispensing port by a micro-pipette. The sample substrate was maintained at around the dew point of the ambient conditions by enclosing the sample substrate with a latex sheet and having wet cotton layers inside the enclosure. This system allowed for extended sample observation time up to one hour without a loss of liquid from the micro-channels.

5. Cells and organelles

Chlamydomonas strains were grown in Tris-acetate-phosphate (TAP) medium prepared as described previously,[30] at a light intensity of 30 to 100 μmol photon m^{-2} s^{-1}, in Erlenmeyer flasks with shaking at 100 to 200 rpm. To facilitate cell capture and penetration of the outer membrane, we utilized the cell wall-deficient, paralysed-flagella Chlamydomonas strains CC-2846 (*arg7cw15pf18*) and CC-2854 (*cw92pf18*). The Chlamydomonas cells generally appear approximately spherical with a diameter of 5–10 μm. The cell has a single cup-shaped chloroplast that can occupy nearly half of the volume of the cytoplasm.

6. System modeling

Capillary flows in micro-fluidic channels were characterized using a MATLAB script (MATLAB 6.5, The Mathworks, Inc.). The flow rate and velocity was calculated for the various geometric conditions of the micro-channels based on eqn (1) to (3). Deionized water was selected as a model fluid and its properties such as surface energy ($\gamma = 70$ mN m^{-1}) and viscosity ($\eta = 1 \times 10^{-3}$ N s m^{-2}) were used in the calculations. Detailed flow patterns around micro-traps were further analysed using a 3D fluidic model by COMSOL Multiphysics 3.2 (COMSOL, Inc, CA). The model was constructed with the incompressible Navier Stokes equations.[31] The viscosity of the liquid was set as 10^{-3} kg ms^{-1} and the density at 10^3 kg m^{-3}. Uniform flow boundary conditions were applied at the entrance of the channel and the mean velocity of the liquid was set as 0.5 mm s^{-1}. The channel width was set as 20 μm with different geometries of the micro-traps. The channel length was set at 100 μm and micro-traps were placed in the middle to allow for full flow development. A non-slip boundary condition was applied at the sidewalls.

Results and discussion

1. Open channel system with traps

Optically transparent PMMA films (50 μm thick) were micro-molded on micro-fabricated silicon wafers, sputtered with gold and then treated with a surfactant, as described in the 'Materials and methods' section, to generate the micro-channel structure shown in Fig. 4. These microstructures were uniform across the PMMA film of 60 × 60 mm^2.

Micro-traps placed in the micro-channels for cell capture were designed after consideration of multiple parameters. In particular, the shape of the micro-traps and the gap between the traps and the wall of the micro-channels were carefully designed since immobilization of the cells depends on the fluidic behavior around the traps. However, micro-molding processes impose a certain limitations on trap design. As the aspect ratio (depth/width or height/width) of a micro-feature becomes larger, demolding of the micro-feature becomes more difficult, often resulting in micro-feature breakage (either polymers or silicon micro-molds). Thus, the shape of the micro-traps was designed to maintain a specific width during demolding, making them resistant to breakage, and a specific geometry that allows appropriate flow regulation. The optimal shape was triangular, with an angle at one side that could be varied to adjust flow patterns. The gap between the micro-trap and the walls of the channels controls the flow resistance of the structure and contributes to the flow pattern around the trap. The gap was varied to achieve various flow patterns, with the narrowest gap of 2 μm in a 5 μm deep channel (aspect ratio of 2.5).

The efficiency of cell immobilization also depends on the capillary force generated by the interaction between the cell solution and the surface of the micro-channels. Although most of the channel surfaces were hydrophilic, the channels were not able to elicit capillary flow. This reflects an open channel structure in which there is no surface tension contribution from the open side of the channel. Therefore, we treated the gold surface coating (which acts as counter-electrode) of the PMMA layers of the channel with a strong hydrophilic surfactant, PEG-thiol.[32] This surface treatment enhanced capillary flow of the introduced solution, allowing for instantaneous filling of the full length of the micro-channels. The contact angle of the PEG-thiol treated surface was 30°, while the bare surface or gold-sputtered surface of PMMA had the contact angles of 90° and 45°, respectively.

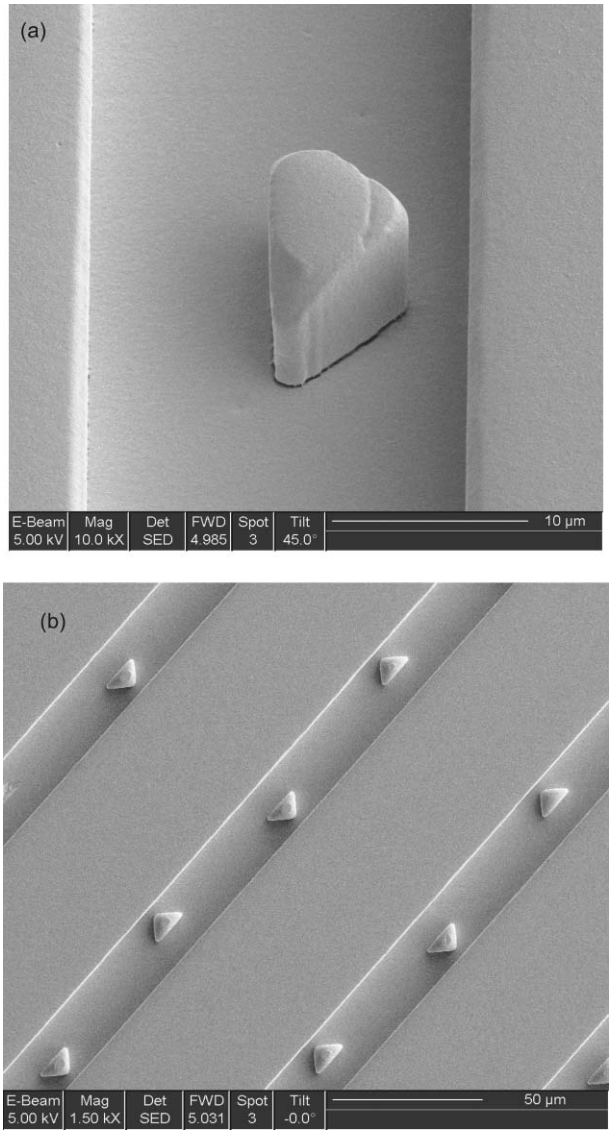

Fig. 4 SEM images of open channel traps on PMMA sheets. (a) Triangular micro-trap with a gap of 3 μm between the right-hand wall and the trap structure. (b) Multiple traps in parallel micro-channels. The channels are 20 μm wide.

The PMMA-based micro-fluidic system has many advantages for our investigations. As AFM manipulated probing is performed with cells that have been immobilized by the trap structures in the channels, it is critical to be able to view the cells at the same time as the manipulations are being performed. Most microscopes used for AFM are inadequate for viewing biological samples, particularly those immersed in an aqueous environment. The most effective viewing of the cells can be

achieved with an inverted microscope, which requires that the substrate used to capture the target cells be optically transparent. The PMMA layers are optically transparent even when coated with thin layers of gold and PEG-thiol, which is unlike the micro-fluidic systems constructed from silicon. The ultra-thin nature of the PMMA layers also allows the high resolution imaging by the inverted microscope up to 100 times of magnification. The low cost of fabrication is another advantage of our system. A single micro-molding, which only takes a few minutes, generates eight sets of the system. Furthermore, a single channel set has multiple sites at which individual cells could be immobilized for making electrochemical measurements; this facilitates the generation of replicate sets of data, Furthermore, PMMA is biocompatible and does not harm the cells during the experiments. Finally, this process is not limited to PMMA, but can be expanded to any thermoplastic material.

2. Capillary flow in open micro-channels

Once a cell solution is dispensed into a reservoir port of an open channel system, an immediate, strong capillary flow occurs. Most of the cells are carried into micro-channels by this initial flow and are sequentially immobilized in the micro-traps. The capillary flow then typically slows down and stops when the front end of the solution arrives at the empty reservoir on the other side. The organization and immobilization of cells occur during this early flow, making the efficiency of cell immobilization dependent upon the flow rate through the micro-channels and the flow pattern around the micro-traps.

We analysed the flow behavior in open micro-channels with varying dimensions using MATLAB software. This flow is described as eqn (1) to (3). Fig. 5(a) shows that the flow rate is high at the channel entrance and decreases gradually as the flow front moves further downstream. This decreased rate is due to increasing flow resistance (R_{fr}), as expressed in eqn (3). Regardless of the location of the flow front, the capillary force as a driving force is constant as long as the geometry of the micro-channels does not change. However, the resistance increases linearly since the volume of flow that the constant capillary force must carry increases as the flow moves further downstream. Eventually, the flow travels over a certain distance and stops when capillary force is balanced by flow resistance. The cross-sectional dimensions of the micro-channels also affect the behavior of the capillary flow. As shown in Fig. 5(b), the flow rate of the capillary increases as the channel depth or width increases. Interestingly, the velocity of the flow front increases as a channel becomes deeper, but only to a certain depth (Fig. 5(c)). This means that the filling time of a channel becomes less sensitive to a change in channel depth above a certain depth threshold. We chose 20 μm as the optimal width of the micro-channels since our target cell, Chlamydomonas, has a diameter of 5 to 10 μm. The depths of the channels used for our experiment were 5, 8, and 10 μm.

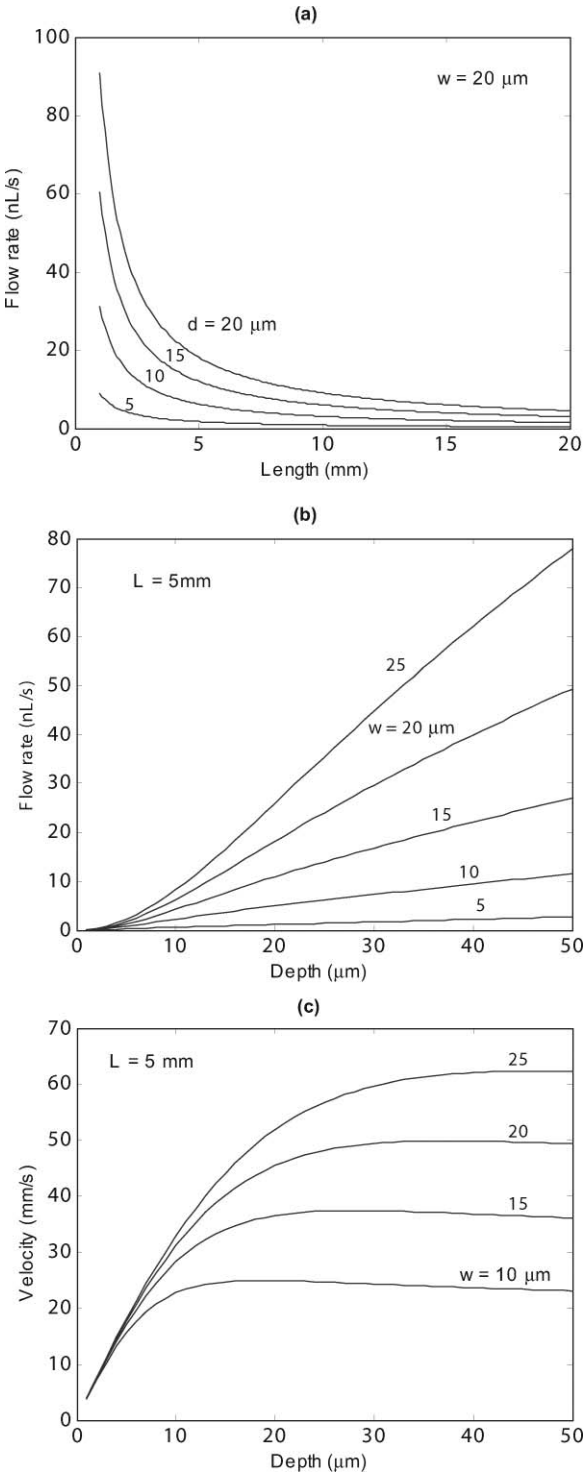

Fig. 5 Characteristics of open micro-channel flow under various geometric conditions.

3. Design of micro-traps

The flow pattern around the micro-traps was simulated using the COMSOL simulation package. The main goal of the simulation was to find the optimal size of the gap between the trap and channel wall. It is important to have a certain amount of flow go through this gap (gap flow), while the size of the gap must be small enough to capture the cell, which would completely block further fluid movement through the gap. As shown in Fig. 6, the size of the gap was varied from 1 and 5 μm for a fixed bypass width of 10 μm and the corresponding flow patterns were analysed. A flux ratio was defined as the ratio of flow through the gap over the total flow through a channel. The flux ratio

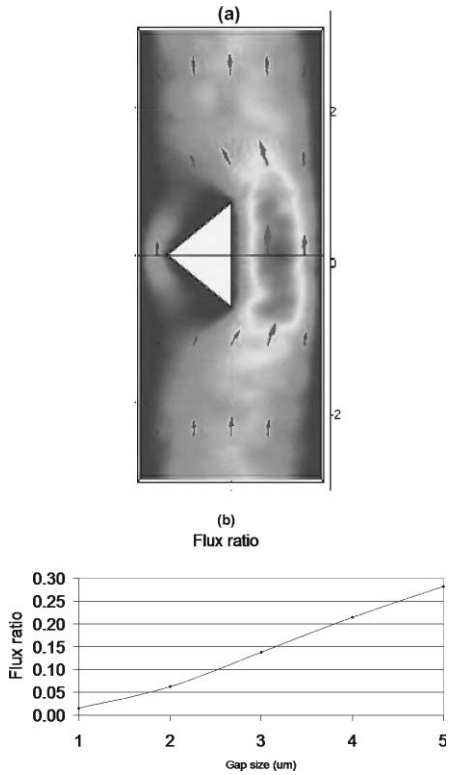

Fig. 6 Finite element analysis of flow pattern for design of optimal micro-traps.

increases from below 2% to about 30% of the total flux as the gap increases from 1 to 5 μm. This flux ratio indicates the probability of trapping cells in a channel. Thus, it is desired to increase the trapping probability by making the gap as large as possible, but not so large that it allows for the passage of the target cell. Based on this analysis, a 3 μm gap size was selected as optimal for our micro-traps.

4. Trapping cells and AFM probing

A droplet of a solution (3–5 μL) containing non-motile (paralysed-flagella) Chlamydomonas cells was dispensed at one end of the open micro-channel structure. Autonomous capillary flow was initiated, which carried the cells along the channels. The cells were captured by micro-traps in the channels and immobilized by the pressure gradient generated from continuous capillary flow, as shown in Fig. 7. Once a cell is positioned in a trap, other cells flowing through the channel pass around the occupied traps; no aggregation of cells in the trap structures was observed. The final product was an array of trapped, single cells in multiple micro-channels, which allows for the sequential probing of multiple cells without reinitiating the trapping process. Even after the capillary flow stopped, the cells stayed at the trap since the cells were mechanically anchored between the trap and wall of the channel. The cells remained trapped until the end of an experiment for up to 50 minutes. Furthermore, the cell solution was contained in the micro-channels (5 to 10 μm deep), guaranteeing that cells were always immersed in an aqueous environment. However, the shallow liquid layer minimizes immersion of the nano-probe, which reduced the parasitic capacitance by five orders of magnitude (from

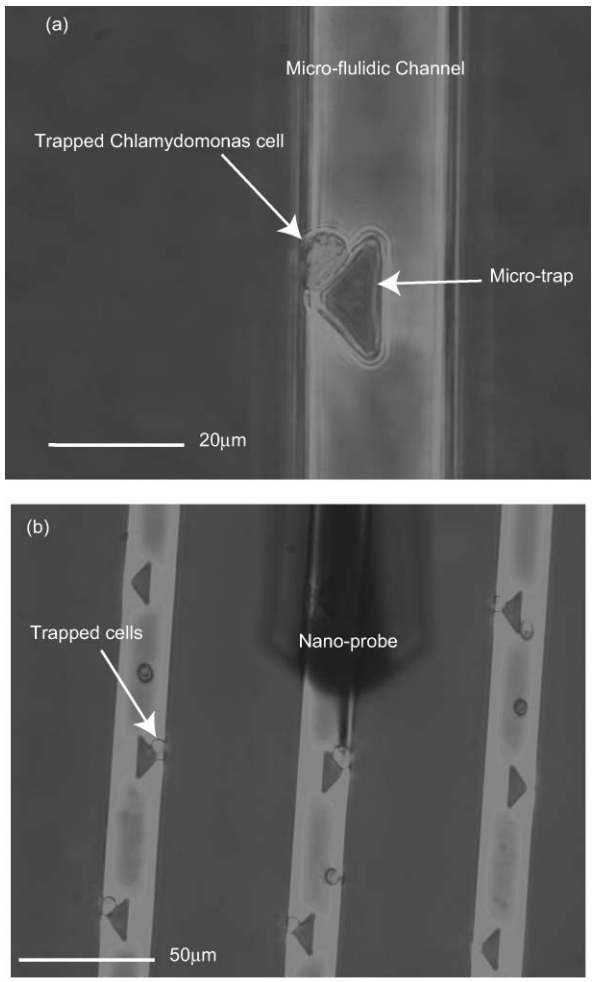

Fig. 7 (a) Optical image of Chlamydomonas trapped in an open channel platform mounted on top of thin cover glass. (b) Individual Chlamydomonas cells are captured at multiple micro-traps. A cell is being penetrated by AFM-operated nano-probes for monitoring of electrochemical responses to light absorption. The images were taken under 100× and 40× magnification from below the micro-fluidic platform.

0.55 nF to 5.5 fF), allowing for electrochemical measurement in the current range of sub-pA. The micro-fluidic and AFM system was kept inside a closed chamber with a relative humidity that was maintained at around 90% in order to prevent evaporative losses of the cell solution. Each experiment could be performed for up to an hour without compromising cellular function.

Once cells were immobilized in the micro-traps, the nano-probe tip was positioned on the surface of the cells by AFM manipulation and further *z*-direction pressure was applied by nano-metre scale movement, which allowed penetration of the target cells. In addition, the ability to position and move the nano-probe within the cell is expected to enable the detection of currents associated with specific subcellular structures in future experiments. In the present experiment, we aimed to locate the nano-probe proximal to the thylakoid stacks within chloroplasts, a region within the chloroplast associated with the generation of high potential electrons. Penetration of the nano-probe into chloroplasts within Chlamydomonas cells was

reliably performed, while the positioning of the nano-probe close to thylakoid stacks requires further investigation.

5. Electrochemical measurement

A gold nano-probe was inserted in a single Chlamydomonas cell followed by illumination of the cells with cold light (halogen light, Carl Zeiss HAL 100, filtered by hot mirror). Polarizing the probe electrode relative to a gold counter electrode that was patterned onto the micro-fluidic substrate, yielded oxidation currents. Currents were dependent on light intensity (larger currents were generated with more intense light), with a maximal intensity used of 108 μmol photon m^{-2} s^{-1}. About 1 pA of oxidation current was observed at a voltage bias of 200 mV, as shown in Fig. 8. The source of this signal was verified using a green light filter (D546/4 green band pass filter, Chroma Technologies, Rockingham, VT), which passes through only wavelengths between 544 and 548 nm and blocks out wavelengths of light that stimulate photosynthetic electron flow and also eliminates the oxidation current. Potential electron donors responsible for current generation are the thylakoid-associated plastoquinone pool and ferredoxin, a peripheral membrane protein that associates with photosystem I on the stromal side of the thylakoid membranes.[33,34] These oxidation signals represent interactions of the electrode with primary targets for studying *in vivo* energy conversion processes in photosynthetic cells. Further investigation is required to verify the source of the observed relation between light intensity and current.

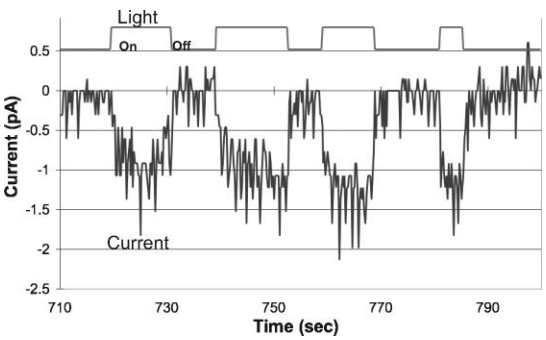

Fig. 8 Oxidation current at a nano-probe potential of 200 mV in respect to Au quasi-reference electrode.

Conclusions

An open micro-fluidic channel system has been developed for electrochemical AFM probing of the unicellular algal cells or chloroplasts isolated from plant cells. The micro-fluidic system employs micro-traps and capillary flow to immobilize individual cells in an arrayed configuration for easy access of the AFM manipulated probe, reduction of leakage currents, and controlled micro-environments that sustain cellular activities. Cells of 5 to 10 μm in diameter were successfully immobilized in these micro-fluidic structures. Once single cells were trapped, nano-electrodes could be positioned on the surface of the cell, with subsequent penetration of the electrode into the cell allowing for the measurement of light-dependent oxidation currents. The configuration of the micro-fluidic structures allowed for AFM probings of a number of different cells without changing the experimental substrate. Furthermore, the parasitic capacitance of the system was markedly reduced by minimizing the area of the probe that was wetted by the solution within the channel. This reduction in parasitic capacitance enabled electrochemical measurements in the sub-pA current range. Overall, the combined use of the nano-electrode and micro-fluidic open channel structures provides a novel platform for *in situ* investigations of the reactions associated with photosynthesis and other electrochemical processes in living cells.

Acknowledgements

This work was supported by the Global Climate and Energy Project at Stanford University.

References

1 R. E. Blankenship, *Molecular Mechanisms of Photosynthesis*, Blackwell Scientific, Oxford, UK, 2002.
2 A. A. Bulychev, V. K. Andrianov, G. A. Kurella and F. F. Litvin, *Nature*, 1972, **236**, 175–177.
3 A. A. Bulychev, V. F. Antony and E. V. Schevchenko, *Biochim. Biophys. Acta*, 1992, **1099**, 16–24.
4 R. J. Fasching, Y. Tao and F. B. Prinz, *Sens. Actuators, B*, 2005, **108**, 964–972.
5 S.-J. Bai, T. Fabian, F. B. Prinz and R. Fasching, *Sens. Actuators, B*, 2008, **130**, 249–257.
6 P. Sun, F. O. Laforge, T. P. Abeyweera, S. A. Rotenberg, J. Carpino and M. V. Mirkin, *Proc. Natl. Acad. Sci. U. S. A.*, 2008, **105**, 443–448.
7 C. Vilchez, I. Garbayo, E. Markvcheva, F. Galvan and R. Leon, *Bioresour. Technol.*, 2001, **78**, 55–61.
8 A. R. Wheeler, W. R. Throndset, R. J. Whelan, A. M. Leach, R. N. Zare, Y. H. Liao, K. Farrell, I. D. Manger and A. Daridon, *Anal. Chem.*, 2003, **75**, 3581–3586.
9 W.-H. Tan and S. Takeuchi, *Proc. Natl. Acad. Sci. U. S. A.*, 2007, **104**, 1146–1151.
10 D. D. Carlo, L. Y. Wu and L. P. Lee, *Lab Chip*, 2006, **6**, 1445–1449.
11 P. Sabounchi, C. Ionescu-Zanetti, R. Chen, M. Karandikar, J. Seo and L. P. Lee, *Appl. Phys. Lett.*, 2006, **88**, 183901.
12 P. J. Lee, P. J. Hung, R. Shaw, L. Jan and L. P. Lee, *Appl. Phys. Lett.*, 2005, **86**, 223902.
13 M. Deutsch and A. Weinreb, *Cytometry*, 1994, **16**, 214–226.
14 M. Khine, A. Lau, C. Ionescu-Zanetti, J. Seo and L. P. Lee, *Lab Chip*, 2005, **5**, 38–43.
15 A. Y. Lau, P. J. Hung, A. R. Wu and L. P. Lee, *Lab Chip*, 2006, **6**, 1510–1515.
16 I. Biran and D. R. Walt, *Anal. Chem.*, 2002, **74**, 3046–3054.
17 J. A. Shapiro and C. Hsu, *J. Bacteriol.*, 1989, **171**, 5963–5974.
18 K. C. Neuman, E. H. Chadd, G. F. Liou, K. Bergman and S. M. Block, *Biophys. J.*, 1999, **77**, 2856–2863.
19 W. D. Donachie and K. J. Begg, *Nature*, 1970, **227**, 1220–1224.
20 E. Ostuni, C. S. Chen, D. E. Ingber and G. M. Whitesides, *Langmuir*, 2001, **17**, 2828–2834.
21 J. Gao, X. F. Yin and Z. L. Fang, *Lab Chip*, 2004, **4**, 47–52.
22 J. Voldman, M. L. Gray, M. Toner and M. A. Schmidt, *Anal. Chem.*, 2002, **74**, 3984–3990.
23 R. A. Flynn, A. L. Birkbeck, M. Gross, M. Ozkan, S. Bing, M. M. Wang and S. C. Esener, *Sens. Actuators, B*, 2002, **87**, 239–243.
24 M. Deutsch, A. Deutsch, O. Shirihai, I. Hurevich, E. Afrimzon, Y. Shafran and N. Zurgil, *Lab Chip*, 2006, **6**, 995–1000.
25 C. Rotsch, K. Jacobson and M. Radmacher, *Proc. Natl. Acad. Sci. U. S. A.*, 1999, **96**, 921–926.
26 E. A-Hassan, W. F. Heinz, M. D. Antonik, N. P. D'Costa and S. Nageswaran, *Biophys. J.*, 1998, **74**, 1564–1578.

27 D. Juncker, H. Schimid, U. Drechsler, H. Wolf, M. Wolf, B. Michel, N. Rooji and E. Delamarche, *Anal. Chem.*, 2002, **74**, 6139–6144.
28 J. P. Hartnett and M. Kostic, in *Advances in Heat Transfer*, Academic Press, New York, 1989, vol. 19, pp. 247–356.
29 W. Ryu, R. Fasching, M. Vyakarnam, R. S. Greco and F. B. Prinz, *J. Microelectromech. Syst.*, 2006, **15**, 1457–1465.
30 E. H. Harris, *The Chlamydomonas Sourcebook*, Academic Press, San Diego, 1989.
31 F. M. White, *Fluid Mechanics*, McGraw-Hill, Inc, New York, 1994.
32 A. Papra, A. Bernard, D. Juncker, N. B. Larsen, B. Michel and E. Delmarche, *Langmuir*, 2001, **17**, 4090–4095.
33 D. Marchal, W. Boireau, J. M. Laval, C. Bourdillon and J. Moiroux, *J. Electroanal. Chem.*, 1998, **451**, 139–144.
34 P. Jordan, P. Fromme, H. T. Witt, O. Klukas, W. Saenger and N. Krauss, *Nature*, 2001, **411**, 909–917.